EPJ manuscript No.
(will be inserted by the editor)

Avoiding traps in trajectory space: metadynamics enhanced transition path sampling

Ernesto E. Borrero and Christoph Dellago[a]

Faculty of Physics, University of Vienna, Sensengasse 8, 1090 Vienna, Austria

Abstract. We propose a transition path sampling (TPS) scheme designed to enhance sampling in systems with multiple reaction channels. In this method, based on a combination of the metadynamics algorithm with the TPS shooting move, a history dependent bias drives the simulation towards unexplored reaction channels. The bias, constructed as a superposition of repulsive Gaussian potentials deposited on the trajectories harvested in the course of the simulation, acts only during the initial stage of the trajectory generation, but leaves the dynamics along the trajectories unaffected such that the sampled pathways are true dynamical trajectories. Simulations carried out for two test systems indicate that the new approach effortlessly switches between distinct reaction channels even if they are separated by high barriers in trajectory space.

1 Introduction

During the past decades, path based computer simulation approaches [1–9] have contributed significantly to a better understanding of many important condensed phase processes, ranging from protein folding to chemical reactions and phase transitions [10]. The dynamics of such systems are often characterized by rare transitions over high free energy barriers separating long-lived stables states. Path sampling methods such as milestoning [1], forward flux sampling [2], the string method [3] or transition path sampling [5,6,9] address the resulting time scale problem by concentrating the computational effort on those segments of the system's time evolution during which the rare transition event occurs, thus avoiding long waiting times between these events. Transition path sampling (TPS), for instance, is based on the statistical definition of an ensemble of pathways that includes only trajectories connecting the stable states of interest and excluding all others. Trajectories from this transition path ensemble are then sampled using a Markov chain Monte Carlo procedure that guarantees that trajectories are harvested according to their correct statistical weight.

While the various path based rare events methods differ in the specific way used to enforce the sampling of reactive trajectories, they are all prone to sampling problems if the transition can occur through different channels separated from each other in trajectory space by high energy or entropy barriers. In this case, the sampling may

[a] e-mail: christoph.dellago@univie.ac.at

remain confined to one of the transition mechanisms while leaving the other channels unexplored even if they are equally or even more important. As a Monte Carlo method, however, transition path sampling can be easily combined with enhanced sampling algorithms developed previously for conventional Monte Carlo simulations. For instance, parallel replica [11–16] and Wang-Landau sampling [17,18] have been used to overcome sampling problems associates to high energy barriers in the trajectory space, improving the switching between pathways passing through distinct reaction channels.

In this work, we present a new approach for enhanced sampling of trajectory space, denoted MetaTPS, which exploits the basic idea of the metadynamics algorithm [19–23], a powerful computational method developed to explore the configuration space of complex systems with metastable states. In a conventional metadynamics simulation, a history-dependent bias potential, acting on some suitably selected collective variables, drives the system away from configuration space regions that have been visited before. As the metadynamics simulation proceeds, this bias effectively fills up free energy basins thus coercing the system to cross otherwise insurmountable barriers into unexplored territory. Here, we harness this concept of a time-dependent bias to enhance the sampling efficiency of transition path sampling simulations and increase the rate at which qualitatively new pathways are harvested. The bias accumulated in the course of the path sampling simulation is applied during the generation of a new trajectory from an old one in a way that affects the TPS simulation only at the Monte Carlo level but leaves the dynamics along the trajectory unchanged. Thus, trajectories sampled with MetaTPS are true dynamical trajectories that faithfully reflect the unbiased intrinsic time evolution of the system during the transition event. The algorithm only alters the statistical weight of individual trajectories in the course of the simulation, suppressing trajectory space regions visited before and favoring exploration of new pathways.

2 Algorithm

In the following, we will briefly review the TPS formalism in order to set the stage for the introduction of the MetaTPS scheme. In essence, TPS is an importance sampling procedure in trajectory space designed to harvest dynamical trajectories connecting two given long-lived states, A and B, defined as regions in configuration space. Pathways are sampled according to their probability to occur, which, for Markovian dynamics, can be expressed as a product of short-time transition probabilities. The algorithm is based on the iteration of a basic step, in which first a new pathway, $x^{\mathrm{n}}(\tau)$, is created from an old one, $x^{\mathrm{o}}(\tau)$, and then the new path is accepted or rejected [6]. Here, τ denotes the temporal length of the pathways and the superscripts o and n refer to the old and new path, respectively. Each pathway is represented by a discrete set of L time slices $x_{t'} = \{q_{t'}, p_{t'}\}$ separated by equal time intervals Δt and each including the positions q and momenta p of all N particles in the system.

An efficient way to generate a new pathway, called the shooting move, consists in selecting a time slice $x^{\mathrm{o}}_{t'}$ on the current trajectory $x^{\mathrm{o}}(\tau)$ [4,24]. Then, this shooting point is modified by addition of a small perturbation δx,

$$x^{\mathrm{n}}_{t'} = x^{\mathrm{o}}_{t'} + \delta x. \tag{1}$$

Typically, the perturbation is applied only in momentum space by adding random momentum displacements for each degree of freedom, but changes in configuration space are possible as well. Note that in the case of stochastic dynamics (such as Langevin or Brownian dynamics) this modification step can be omitted. From the

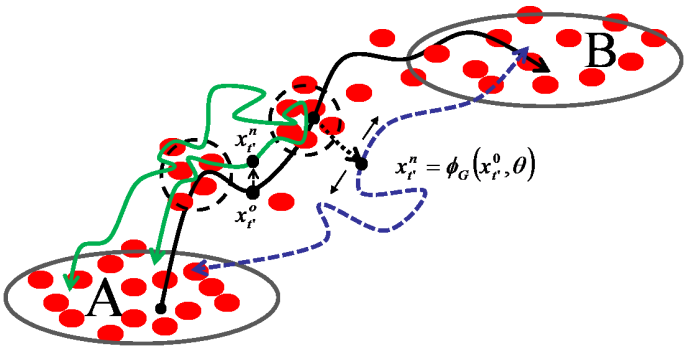

Fig. 1. Schematic illustration of the MetaTPS scheme. To generate a new trajectory (blue dashed line) from the current trajectory (black), the selected time slice $x^{\mathrm{o}}_{t'}$ is first propagated for a time θ under the influence of the time-dependent bias $\mathcal{V}_G$ to obtain the shooting point $x^{\mathrm{n}}_{t'}$. Starting from this point, the new trajectory is determined by integrating the equations of motion forward to time $t = \tau$ and backward to time $t = 0$ without the bias potential such that the new trajectory follows the natural dynamics of the system. If the new trajectory connects the stable states A and B, it is accepted. Otherwise, it is rejected (the green trajectory, for instance, is rejected, because both the forward and the backward trajectory segments reach stable region A). The filled, red circles indicate Gaussian repulsive potentials that have been deposited in the space spanned by the collective variables in the course of the simulation, and the dashed circles represent metastable regions in which the system may get trapped on its way from A to B.

modified shooting point at time t' the equations of motion are then integrated forward to time τ and backward to time 0. The new trajectory $x^{\mathrm{n}}(\tau)$ obtained in this way is then accepted if it connects the initial with the final region and rejected otherwise [24]. Iteration of this shooting move typically leads to rapid decorrelation in trajectory space such that a statistically independent pathway is obtained after few accepted moves.

In situations in which the transition can occur via different, well separated reaction channels, however, a straightforward application of the shooing algorithm may miss important mechanisms during the available simulation time. To increase the sampling rate and prevent the TPS simulation from getting trapped in a specific reaction channel, we generalize the basic concepts of metadynamics to trajectory space and introduce a history-dependent bias $\mathcal{V}_G$ accumulated during the TPS simulation. More specifically, the bias $\mathcal{V}_G(q, i_{\mathrm{MC}})$ acting on a particular configuration q is constructed as a sum of repulsive Gaussians positioned at configurations q_k collected from trajectories sampled previously,

$$\mathcal{V}_G(q, i_{\mathrm{MC}}) = w \sum_{k=1}^{N_G(i_{\mathrm{MC}})} \exp\left\{ -\sum_{j=1}^{d} \frac{[s_j(q) - s_j(q_k)]^2}{2\delta_{s_j}^2} \right\}. \tag{2}$$

Here, $N_G(i_{\mathrm{MC}})$ is the total number of Gaussians accumulated up to iteration i_{MC} of the TPS procedure, and w and δ_{s_j} denote the height and width of the Gaussians, respectively. The configurations q_k are gathered from previous pathways at regular time intervals τ_G such that after i_{MC} TPS steps a total of $i_{\mathrm{MC}}\,\tau/\tau_G$ Gaussian potentials have been deposited. As in metadynamics, the bias depends on the configuration q through a set of collective variables $S = \{s_1(q), s_2(q), \cdots, s_d(q)\}$ that need to be selected in advance depending on the particular situation under study. These

collective variables have to be carefully chosen such that they distinguish among multiple metastable states (stable and intermediates) and describe all the slow events occurring during the transition connecting the two stable states. In MetaTPS it is particularly important that the collective variables do not only capture metastability along transition pathways but also orthogonal to them, such that the bias can drive switches between different reaction channels. Typical collective variables that have been successfully used in metadynamics applications include global properties such as the potential energy of the system and more local, system-specific geometric variables such as angles, local bond order parameters and coordination numbers [21, 25]. In addition to these configurational features, path properties such as the distance from a reference path or from previous pathways [26] also lend themselves for use in the MetaTPS approach.

The bias built up over time is then used in the generation of the new shooting point $x^{\rm n}_{t'}$ from a point $x^{\rm o}_{t'}$ selected randomly with uniform probability along the current pathway $x^{\rm o}(\tau)$. The new shooting point is obtained by propagating the system for a time θ under the influence of the time dependent potential $\mathcal{V}_G$,

$$x^{\rm n}_{t'} = \phi_G(x^{\rm o}_{t'}, \theta), \tag{3}$$

by carrying out an appropriate number of molecular dynamics steps. Here, ϕ_G is the system's propagator with the bias potential on. Note that an extra perturbation may be added to the selected time slice $x^{\rm o}_{t'}$ before carrying out the biased integration in order to enhance the trajectory generation during the initial simulation stages when the external bias $\mathcal{V}_G$ is weak.

Once the shooting point $x^{\rm n}_{t'}$ has been constructed using this procedure, one proceeds as in a conventional TPS simulation and generates the new trajectory by integrating forward and backward in time from $x^n_{t'}$ by applying the appropriate dynamical rules, without bias. The newly generated pathway is then accepted with a probability $P_{\rm acc}$ that depends on the relative phase space weights $\rho(x^o_{t'})$ and $\rho(x^n_{t'})$ and on whether the new trajectory connects stable states A and B,

$$P_{\rm acc}\left[x^{\rm o}(\tau) \to x^{\rm n}(\tau)\right] = h_A(x^{\rm n}_0) H_B[x^{\rm n}(\tau)] \min\left[1, \frac{\rho(x^{\rm n}_{t'})}{\rho(x^{\rm o}_{t'})}\right]. \tag{4}$$

In the above equation, $h_A(x)$ is the characteristic function for region A, which equals unity if x is inside A and is zero otherwise, and $H_B[x^{\rm n}(\tau)] = \max_{0\le t\le\tau} h_B(x_t)$ is unity if the path $x(\tau)$ visits region B and vanishes otherwise.

A variation of the algorithm consists in taking into account the time dependent bias also in the acceptance steps, leading to

$$P_{\rm acc}\left[x^{\rm o}(\tau) \to x^{\rm n}(\tau)\right] = h_A(x^{\rm n}_0) H_B[x^{\rm n}(\tau)] \min\left[1, \frac{\rho(x^{\rm n}_{t'})}{\rho(x^{\rm o}_{t'})}\frac{\mathcal{W}_G(x^{\rm o}_{t'})}{\mathcal{W}_G(x^{\rm n}_{t'})}\right], \tag{5}$$

where $\mathcal{W}_G(x) = \exp\{-\beta\mathcal{V}_G(x, i_{\rm MC})\}$ is the Boltzmann factor corresponding to the bias potential accumulated after $i_{\rm MC}$ TPS iterations. This equation results from the fact that the probability $p_{\rm gen}(x^{\rm n}_{t'} \to x^{\rm o}_{t'})$ to generate the new shooting point under the effect of the repulsive $\mathcal{V}_G$ potential accumulated up to i_{MC} is related to the probability $p_{\rm gen}(x^{\rm o}_{t'} \to x^{\rm n}_{t'})$ of the reverse generation move by microscopic reversibility [6],

$$\frac{p_{\rm gen}(x^{\rm n}_{t'} \to x^{\rm o}_{t'})}{p_{\rm gen}(x^{\rm o}_{t'} \to x^{\rm n}_{t'})} = \frac{\mathcal{W}_G(x^o_{t'})}{\mathcal{W}_G(x^n_{t'})}. \tag{6}$$

Although this alternative acceptance algorithm yields similar results as the one described by Equ. (4), we do not consider it further in this paper.

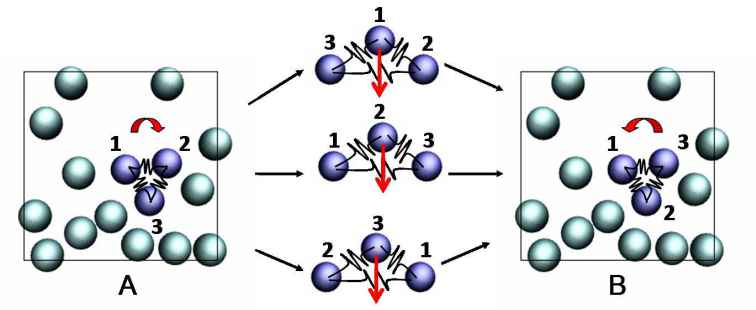

Fig. 2. The triatomic molecule in two dimensions, immersed in a bath of soft disks, can exist in two stable configurations, in which the atoms are arranged clockwise (A) and counter-clockwise (B). Transitions between states A and B can occur via three distinct but equivalent reaction channels illustrated in the column at the center. Arrows indicate the motion of the atoms during the transition.

A schematic representation of the shooting move carried out in the MetaTPS algorithm is shown in Fig. 1. Note that the bias accumulates preferentially in the highly visited regions. A shooting point selected in these regions is then quickly driven away from the current trajectory. The perturbation of the shooting point is smaller away from the highly visited regions such that in that case the new pathway more closely resembles the old one.

3 Illustrative applications

3.1 Triatomic molecule in solvent

To illustrate the MetaTPS approach we now apply it to a structural transition with multiple reaction channels. The system, shown schematically in Fig. 2, consists of a triatomic molecule in two dimensions, in which the atoms are connected by harmonic springs with interaction potential

$$V_H(r) = \frac{h}{2}(r - R)^2. \tag{7}$$

Here, r is the interatomic distance and h and R denote the spring constant and the equilibrium bond length, respectively. The molecule is immersed in a fluid of purely repulsive disks interacting via the Weeks-Chandler-Andersen potential [27],

$$V_{\mathrm{WCA}}(r) = \begin{cases} 4\varepsilon[(\frac{\sigma}{r})^{12} - (\frac{\sigma}{r})^{6}] + \varepsilon & \text{for } r \leq 2^{1/6}\sigma, \\ 0 & \text{for } r > 2^{1/6}\sigma, \end{cases} \tag{8}$$

where ε and σ determine the strength and the range of the potential, respectively. Periodic boundary conditions apply. Solvent atoms interact with the atoms of the triatomic molecule also via the WCA potential. The triatomic molecule can reside in two conformations in which the three atoms are arranged clockwise (state A) or counter-clockwise (state B). For sufficiently strong intramolecular interactions and low temperatures, states A and B are long-lived and transitions between them occur only rarely, activated by rare solvent fluctuations. The transition can occur via three distinct but equivalent reaction channels, differing by which particle moves between the other two as indicated in Fig. 2.

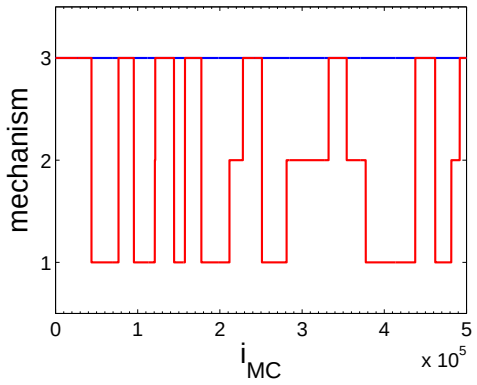

Fig. 3. Transition mechanism observed for the triatomic molecules as a function of the number i_{MC} of TPS iterations. The numbers on the vertical axis refer to the three transition mechanisms indicated in Fig. 2. The blue line shows the results of a regular TPS simulation obtained for $N = 16$ solvent particles at a density of $\rho = 0.6\sigma^{-2}$ and a temperature of $k_{\mathrm{B}}T = 0.5\varepsilon$. The results shown as red line were obtained from a MetaTPS simulation carried out with the same parameters. While the TPS simulation is trapped in one particular reaction channel, the MetaTPS simulation explores all three available mechanisms.

Due to symmetry, all three mechanisms should occur with the same frequency. Conventional transition path sampling simulations, however, are likely to get trapped in one of the transition channels and, hence, may sample only a fraction of the transition path ensemble, as shown exemplarily in Fig. 3. Here, the blue curve indicates the mechanism observed in the TPS simulation as a function of the TPS iterations (numbering of the mechanism as indicated in Fig. 2). Simulations were carried out for $N = 16$ solvent particles at density $\rho = 0.6\sigma^{-2}$ and temperature $k_{\mathrm{B}}T = 0.5\varepsilon$ with a spring constant and equilibrium bond length of the intermolecular interactions set to $h = 20\varepsilon$ and $R = \sigma$, respectively. The paths harvested in the TPS simulations were of length $\tau = 2.0(m\sigma^2/\varepsilon)^{1/2}$ and the equations of motions were integrated using the velocity Verlet algorithm [28] with a time step of $\Delta t = 0.002(m\sigma^2/\varepsilon)^{1/2}$. Shooting points were perturbed by adding momentum displacements for each degree of freedom drawn from a Gaussian distribution with width $\delta = 0.2(m\varepsilon)^{1/2}$. As is clear from Fig. 3, the TPS simulation samples only one (mechanism 3) of the three possible mechanisms and is unable to switch between the three mechanisms in the course of the simulation.

The MetaTPS simulation, on the other hand, samples all three possible mechanisms within the same simulation time, as shown by the red line in Fig. 3. The parameters for the MetaTPS simulation were the same as for the regular TPS run. As only collective variable we used the intramolecular potential energy of the trimer (*i.e.*, the sum of the three harmonic interaction energies between the atoms of the molecule). Following the procedure described above, the new shooting point was obtained by changing only the configurational part of a randomly selected time slice of the old path and propagating the system forward for a time $\theta = 1$ under the influence of the external potential. The momenta of the shooting point were then perturbed by adding random momentum displacements drawn from a Gaussian distribution with width $\delta = 0.2(m\varepsilon)^{1/2}$ as in our conventional TPS run, such that the shooting point is modified even in cases where the history dependent potential $\mathcal{V}_G$ is small in the initial stages of the simulation. The deposition rate of Gaussian bias terms was set to

$\tau_G = 0.02(m\sigma^2/\varepsilon)^{1/2}$ (corresponding to 10 time steps), and their height and width to $w = 1.0\varepsilon$ and $\delta_S = 0.01\varepsilon$, respectively.

Due to the bias building up as the simulation progresses, the sampled trajectories are driven back and forth between the three possible reaction channels (see Fig. 3) and at the end of the simulation consisting of 5×10^5 TPS iterations the fraction of trajectories of type 1, 2, and 3 are 0.22, 0.36, and 0.42, respectively. Even though the time-dependent bias strongly affects the generation of trajectories, the average acceptance probabilities of the TPS and MetaTPS simulations are comparable, having values of 0.14 and 0.10, respectively. As anticipated, the gains in sampling performance vastly outweigh associated acceptance probability decreases.

3.2 Two-dimensional potential energy surface

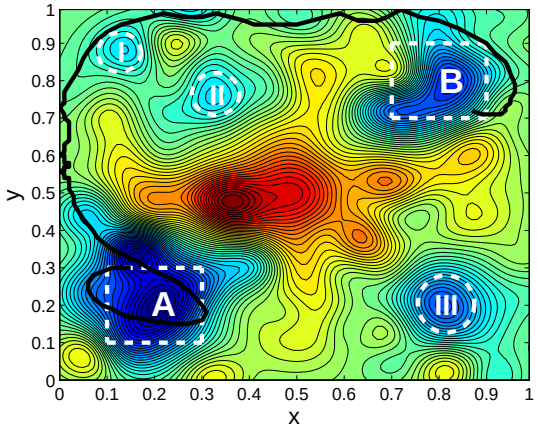

Fig. 4. Contour plot of the two-dimensional potential. The colors change from red for the highest to blue for the lowest energies. The attractive basins, labelled A and B and located at (0.2, 0.2) and (0.8, 0.8), respectively, are enclosed by dashed rectangles. The three intermediate states I, II, and III enclosed by circles are located at (0.12, 0.9), (0.35, 0.75), and (0.8, 0.2). The black line denotes the initial trajectory.

To further test and validate the MetaTPS algorithm we simulated the transition of a single particle moving on a two-dimensional potential energy surface with multiple minima, a system used previously to test other shooting point perturbation algorithms and path sampling methods [29,30]. A contour graph of this rugged energy landscape including the initial trajectory used in our TPS simulations is shown in Fig. 4. The dynamics of the system is governed by the Langevin equation integrated with a time step of $\Delta t = 0.01$ at reciprocal temperature $\beta = 1/k_{\mathrm{B}}T = 10$ for a particle mass of $m = 1.0$ and friction coefficient of $\gamma = 2.5$, all given in reduced units. Reflective boundaries conditions keep the particle inside the region $0 < x < 1$ and $0 < y < 1$. The paths are discretized into $L = 110$ time slices saved at intervals of 10 time steps Δt.

Figure 5 shows density maps obtained from conventional TPS (top) and MetaTPS (bottom) simulations. These density maps, computed by classifying configurations taken from the harvested pathway into a two-dimensional histogram, quantify the frequency with which different regions of configuration space are visited during the

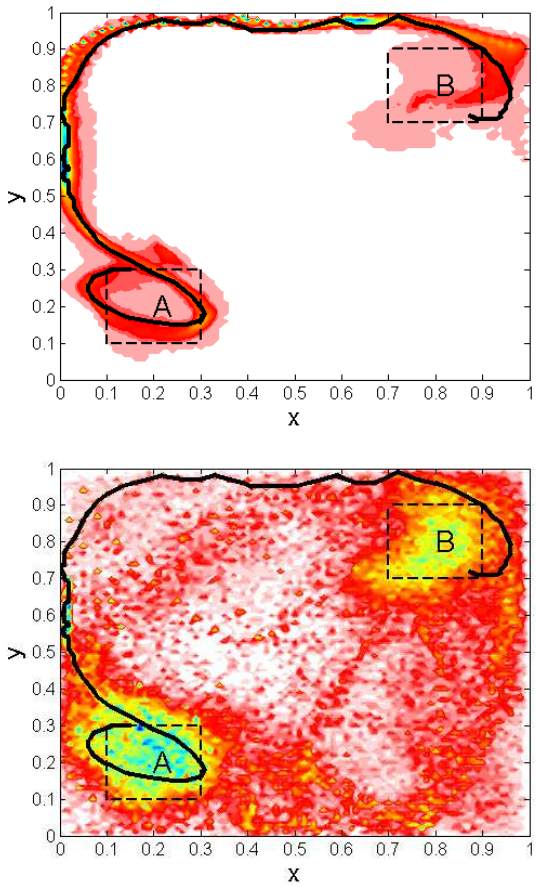

Fig. 5. Density map obtained from transition pathways sampled in a conventional TPS simulation (top) and a MetaTPS simulation (bottom) using x and y coordinates as collective variables. The color scheme changes from most-visited (blue) to non-visited (white) states. The black line denotes the initial trajectory.

transition from A to B. In the TPS simulation, 1×10^5 trajectories of length $\tau = 11.0$ were sampled and the shooting points were perturbed by introducing momentum displacement for each degree of freedom from a Gaussian distribution with width $\delta = 0.25$. Although a large acceptance probability of 0.40 was obtained in this TPS run, the harvested pathways are confined to a narrow channel passing through or near the intermediate state I (see Fig. 4). All other channels, though not less likely, remain unexplored.

Application of the MetaTPS algorithm leads to a much wider distribution of pathways, as can be seen in the bottom panel of Fig. 5. In this simulation, the x and y coordinates have been used as collective variables for constructing the history-dependent potential. The deposition rate of the Gaussian potentials was set to $\tau_G = 0.1$ (10 time steps), and the height and width of the Gaussians to $w = 0.5$ and $\delta_S = 0.01$, respectively. We perturbed the shooting point by changing the positions and momenta part according to Equ. (1) and then propagating the system forward for one time step of length Δt under the influence of the bias $\mathcal{V}_G$. A total of 10^5 trajectories were sampled with an average acceptance probability of 0.2. Due to the time-dependent bias applied

in the MetaTPS scheme switches between different reaction channels occur frequently and all possible transition mechanisms are sampled in the course of the simulation.

Since defining set S of collective variables suitable for the application of the time-dependent bias potential may be far from obvious for many interesting cases, we have also explored the possibility to use general path variables, introduced in the framework of metadynamics [26]. These path variables, specified with respect to a particular reference trajectory, are defined as [26]

$$l_p(q) = \frac{1}{(L-1)} \frac{\sum_{i=1}^{L} (i-1) e^{-\lambda [s(q)-s_i]^2}}{\sum_{i=1}^{L} e^{-\lambda [s(q)-s_i]^2}}, \tag{9}$$

and

$$z_p(q) = -\frac{1}{\lambda} \ln \sum_{i=1}^{L} e^{-\lambda [s(q)-s_i]^2}. \tag{10}$$

Here, L is the number of time slices used to discretize a reference trajectory and s_i denotes the collective variables at time slice i of the reference path. In the above definitions we used the mean squared displacement $[s(q) - s_i]^2$ as measure for the distance in collective variable space between configuration q and the configuration belonging to the respective time slice, but other metrics could be employed as well. The parameter λ controls the smearing out of the reference path and is usually defined to have a magnitude comparable to the inverse of mean square displacement between successive time slices. Thus, $l_p(q)$ and $z_p(q)$ are variables that measure the distance of configuration q along and orthogonal to the reference path, respectively. We carried out a MetaTPS simulation using these two path variables as collective variables. The reference path used to compute the path variables is changed during the simulation in order to drive the simulation to all relevant parts of path space. This is done by periodically replacing the old reference path by the current path and reinitializing the time-dependent bias potential.

A density map obtained from the MetaTPS simulation carried out using the path variables is shown in the top panel of Fig. 6. In this simulation, the reference path was reassigned every 2×10^4 TPS iterations and a total of 10^5 trajectories were collected with an average acceptance probability of 0.2. The deposition rate of Gaussian potentials was $\tau_G = 0.1$ corresponding to 10 time steps, and the height and width of the Gaussians were $w = 0.1$ and $\delta_S = 0.1$ respectively. The five reference paths used in the course of the simulation are shown in the bottom panel of Fig. 6. By harvesting pathways that are driven away from the sequentially updated reference trajectories, the MetaTPS simulation sampled the entire available path space. Since the path variables reduce a possibly high-dimensional collective variable space to two dimensions, these variables seem particularly convenient for the application of the MetaTPS scheme to high-dimensional complex systems, where hundreds of candidate variables may be selected as collective variables for the construction of the history-dependent potential.

4 Conclusion

In summary, the proposed approach, denoted as MetaTPS, can be seen as an iterative procedure where a Gaussian repulsive potential successively fills up valleys in trajectory space corresponding to distinct reaction channels. At early stages of the MetaTPS simulation, the history dependent bias is weak and new trajectories are generated as in regular TPS simulations. As the MetaTPS simulation proceeds, however, the increasing strength of the bias drives the shooting points away from the regions most visited on previously harvested pathways, promoting the generation of

new pathways that strongly diverge from the trajectory they were generated from. As a result, the transition path sampling simulation is driven towards unsampled regions of trajectory space and new reaction channels can be discovered.

For a MetaTPS simulation to be effective, a suitable choice of collective variables is crucial. In regular metadynamics, designed to escape traps in configuration space, the collective variables must be able to distinguish the inital and final state and all meta-stable intermediates between them. Ideally, the collective variables are sufficient to characterize the reaction coordinate, which provides a dynamically meaningful description of the progress of a particular transition. Then, the time-dependent bias drives the system out of long-lived states roughly following the natural transition mechanism. In the path sampling case, however, the metastability may exist in directions orthogonal to the directions of the main reaction channels (for instance, there may be several roughly parallel classes of transition pathways separated by high barriers). A bias only acting in direction of the reaction coordinate would not lead to switches between different reaction channels. Hence, in MetaTPS, one has to make

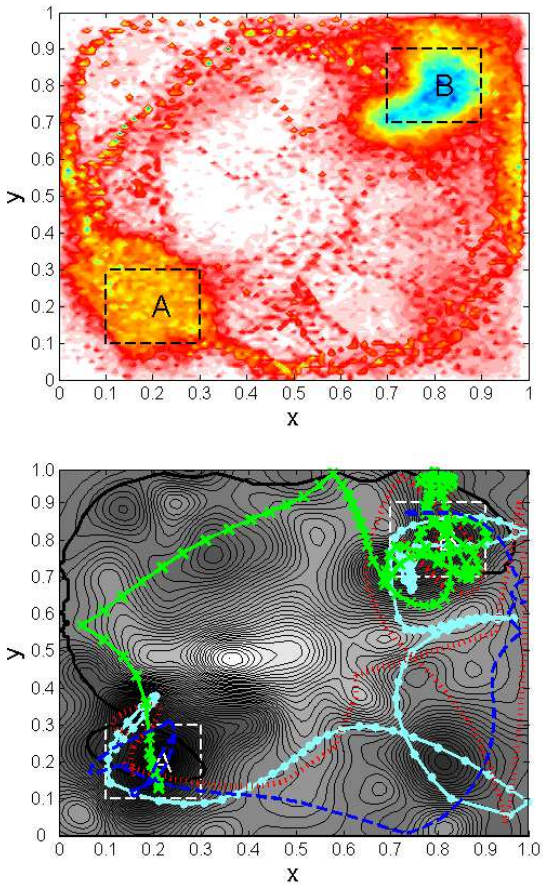

Fig. 6. (Top) Density map obtained from a MetaTPS run using with the path variables defined in Ref. [25] as collective variables. The color scheme for the density map is as in Fig. 5. (Bottom) Reference trajectories used during the MetaTPS simulation superimposed on the contour map of the potential.

sure that the collective coordinates allow to bias the sampling into directions transverse to the transition pathways. If the reaction channels are separated by energetic barriers, the potential energy of the entire system or of parts of the system may provide a collective variable capable of doing that. In fact, in the case of the trimer in solution studied in Sec. 3.1, the potential energy of the trimer was used as collective variable and the associated bias succeeded in inducing transitions between the three classes of transition pathways. Another possibility to drive the pathways in transversal directions is to make the bias dependent on the path collective variables $l_p(q)$ and $z_p(q)$, used in Sec. 3.2, which quantify the distance of a configuration along and orthogonal to a reference path. Including these variable in the biased path generation forces the sampling away from the reference pathway leading to the exploration of new regions in trajectory space.

It is important to note that while the history-dependent bias strongly influences the generation of new shooting points, it leaves the underlying dynamics unaffected such that the harvested pathways are true dynamical pathways following the natural time evolution of the system. Since in a MetaTPS simulation reactivity is maintained at all times (*i.e.*, all trajectories connect the initial with the final region), this approach is very suitable to study rare transitions, such as structural transformations occurring in nanocrystals [31,32], in which other biased sampling approaches would wander off into regions of configuration space unrelated to the transition. Also, the MetaTPS methodology presented in this paper may be used to alleviate problems associated with the generation of the initial transition path needed to start TPS simulations [4]. Repeated application of the MetaTPS move starting from a possibly very unlikely initial pathway accelerates the rate at which the simulation moves towards more typical transition pathways. Finally, by terminating the update of the bias potential once all relevant transition pathway have been sampled, the relative likelihood of the various distinct reaction channels may be estimate in a way analogous to free energy computations in regular metadynamics simulations. An alternative way to exploit metadynamics ideas in the framework of TPS consists in building the effect of the history dependent bias only into the acceptance probability. This approach will be the subject of future investigations.

We acknowledge financial support from Austrian Science Fund (FWF) within the SFB ViCoM (F 41). All simulations presented in this paper were carried out on the Vienna Scientific Cluster (VSC). E.E.B. thanks Davide Branduardi for useful discussions on the metadynamics algorithm.

References

1. A. K. Faradjian and R. Elber, J. Chem. Phys. **120**, 10880 (2004)
2. R. J. Allen, P. B. Warren, and P. R. ten Wolde, Phys. Rev. Lett. **94**, 018104 (2005)
3. W. E, W. Ren, and E. Vanden-Eijnden, J. Phys. Chem. B **109**, 6688 (2005)
4. P. G. Bolhuis, D. Chandler, and C. Dellago, Annu. Rev. Phys. Chem. **53**, 291 (2002)
5. C. Dellago, P. G. Bolhuis, F. S. Csajka, and D. Chandler, J. Chem. Phys. **108**, 1964 (1998)
6. C. Dellago, P. G. Bolhuis, P. L. Geissler, and D. Chandler, Adv. Chem. Phys. **123**, 1 (2002)
7. T. S. van Erp and P. G. Bolhuis, J. Comput. Chem. **205**, 157 (2005)
8. D. Moroni, T. S. van Erp, and P. G. Bolhuis, Phys. A **340**, 395 (2004)
9. P. G. Bolhuis and C. Dellago, Euro. Phys. J. ST **224**, 1 (2015)
10. C. Dellago and P. G. Bolhuis, in *Advanced Computer Simulation Approaches for Soft Matter Sciences III* (Springer, New York, 2009), vol. **221** of *Advances in Polymer Science*, pp.167–233

11. E. Marinari and G. Parisi, Europhys. Lett. **19**, 451 (1992)
12. P. G. Bolhuis, J. Chem. Phys. **129**, 114108 (2008)
13. T. J. H. Vlugt and B. Smit, Phys. Chem. Comm. **4**, 11 (2001)
14. T. S. van Erp, Phys. Rev. Lett. **98**, 268301(2007)
15. T. S. van Erp, Comp. Phys. Comm. **179**, 34 (2008)
16. D. W. H. Swenson and P. G. Bolhuis, J. Chem. Phys **141**, 044101 (2014)
17. F. Wang and D. P. Landau, Phys. Rev. Lett. **86**, 2050 (2001)
18. E. E. Borrero and C. Dellago, J. Chem. Phys. **133**, 134112 (2010)
19. T. Huber, A. E. Torda, and W. F. Gunsteren, J. Comput. Aided. Mol. Des. **8**, 695 (1994)
20. A. Laio and M. Parrinello, Proc. Natl. Acad. Sci. USA **99**, 12562 (2002)
21. A. Laio and F. L. Gervasio, Rep. Prog. Phys. **71**, 126601 (2008)
22. G. Bussi, A. Laio, and M. Parrinello, Phys. Rev. Lett. **96**, 090601 (2006)
23. P. Tiwary and M. Parrinello, Phys. Rev. Lett. **111**, 230602 (2013)
24. C. Dellago, P. G. Bolhuis, and D. Chandler, J. Chem. Phys. **108**, 9236 (1998)
25. D. Provansi, A. Bortolato, and M. Filizola, Biochemistry **48**,10020 (2009)
26. D. Branduardi, F. L. Gervasio, and M. Parrinello, J. Chem. Phys. **126**, 054103 (2007)
27. J. D. Weeks, D. Chandler, and H. C. Andersen, J. Chem. Phys. **54**, 5237 (1971)
28. D. Frenkel and B. Smit, *Understanding Molecular Simulation: From Algorithms to Applications* (Academic, San Diego, CA, 2002)
29. M. Chopra, R. Malshe, A. S. Reddy, and J. J. de Pablo, J. Chem. Phys. **128**,144104 (2008)
30. E.E. Borrero and F. Escobedo, J. Phys. Chem. B **113**, 6434 (2009)
31. M. Grünwald and C. Dellago, Nano Letters **9**, 2099 (2009)
32. M. Grünwald, K. Lutker, A. P. Alivisatos, E. Rabani, and P. L. Geissler, Nano Letters **13**, 1367 (2013)